Surface state effects in high-T_c superconductors

S. H. Liu
Department of Physics, University of California, San Diego, La Jolla, California 92093-0319

R. A. Klemm
Materials Science Division, Argonne National Laboratory, Argonne, Illinois 60439
(Received 6 April 1995)

All copper oxide based high-T_c superconductors share the common property that the c-axis coherence length is shorter than the lattice repeat distance in the same direction. In a semi-infinite system whose top surface is an ab plane, the superconducting properties near the surface may be drastically affected. We report in this paper detailed analyses of the surface properties of model layered superconductors with one and two layers in a unit cell. We have found that for the one-layer model the change in surface electronic structure has no effect on the critical temperature T_c and the order parameter Δ. For a two-layer model with one superconducting (S) layer and one normal (N) layer, the order parameter of the top S layer is generally larger that that of the bulk. The enhancement effect is particularly large when a band of surface state exists on the top S layer. In this event, the energy gap structure measured by the point-contact tunneling technique is expected to be very different from that measured by the junction tunneling technique. Such differences have been reported for $Bi_2Sr_2CaCu_2O_{8+\delta}$ and $YBa_2Cu_3O_{7-\delta}$. The existence of a surface band also adds complications to the interpretation of the photoemission measurements of the superconducting energy gap, to the extent that the observed gap anisotropy may actually reflect the uneven distribution of the spectral weight of the surface state on the top layer. How to extend these findings to systems with three and more layers in a unit cell will also be discussed.

I. INTRODUCTION

Recently, there has been a raging controversy regarding the orbital symmetry of the superconducting order parameter (OP) $\Delta(\mathbf{k})$ in the high transition temperature (T_c) superconductors such as $Bi_2Sr_2CaCu_2O_{8+\delta}$ (BSCCO) and $YBa_2Cu_3O_{7-\delta}$ (YBCO). A number of experiments on these materials were interpreted in terms of $\Delta(\mathbf{k})$ having a $d_{x^2-y^2}$ symmetry such as $\Delta_0(k_x^2-k_y^2)$, with nodes for $k_x=\pm k_y$. Among these are the photoemission experiments of Shen *et al.*,[1] the corner superconducting quantum interference device (SQUID) and Josephson junction experiments of Wollman *et al.*,[2] the tricrystal ring experiments of Tsuei *et al.*,[3] the YBCO/Pb square SQUID experiments of Mathai *et al.*,[4] and the penetration depth λ measurements of Hardy *et al.*[5] In addition, some workers[6–8] have interpreted the different tunneling behaviors observed in point-contact, break junction, and junction measurements on the same and on different sample surfaces as evidence for a d wave, or OP that contains nodes.

On the other hand, c-axis[9] and grain-boundary[10] Josephson tunneling experiments, plus $\mathbf{H}\perp\hat{\mathbf{c}}$ torque measurements[11] were found to be consistent with an isotropic or s-wave OP, $\Delta(\mathbf{k})=\Delta_0$, or possibly with an anisotropic but nodeless OP, such as $s+id$.

All of these experiments are interpreted in terms of the BCS-type theory with an order parameter of s- or d-wave symmetry. This approach is adequate for low-T_c superconductors which have coherence lengths tens or hundreds of times longer than the lattice parameters. It is now known, on the other hand, that in copper oxide based high-T_c superconductors, the c-axis coherence lengths are far shorter than the lattice repeat distances in the same direction. This fact has led us to investigate in microscopic detail the possible effects of the nonsuperconducting layers in these materials on their bulk superconducting properties.[12–16] Based on a two-layer S-N model, we have shown that the intervening N layers can change the critical temperature, the order parameter, the temperature dependence of the penetration depths in a,b directions, and the structure of the density-of-states curve in ways that mimic the effects of d-wave superconductivity. In the course of this study, we discovered that the modified electronic structure on and near the top ab plane of a semi-infinite layered system may profoundly affect its local superconducting properties,[15] such that in case a band of surface states is formed, the superconducting energy gap can be much enhanced. The effect is much stronger than what has been discussed in literature in terms of the Ginzburg-Landau model.[17,18] The predicted gap structure can account for the observed differences in the c-axis point-contact and junction tunneling results.[6–8]

This paper provides details of our analyses reported in Ref. 15 on the surface effects of semi-infinite layered superconductors. In Sec. II we discuss the model with only one S layer and no N layer in a unit cell. The result is trivially simple, i.e., that the change of the electronic structure at the surface has no effect on superconductivity. Yet, the analysis leading to this result is not simple. The mathematical procedure paves the way for the nontrivial two-layer S-N model analyzed in Sec. III, with emphasis on the effects of surface states on superconductivi-

ty and related phenomena. In Sec. IV we extend our consideration to more complex models with three and four layers per unit cell so we can draw physical conclusions about real materials, which is the content of Sec. V.

II. THE ONE-LAYER MODEL

We discuss in this section the superconducting properties of the semi-infinite layered solid with one superconducting layer per unit cell. Section II A reviews the bulk superconducting properties we have published earlier, II B shows how the normal-state electronic structure is solved in the normal state, and II C carries the calculation one step further to the superconducting state.

A. Bulk superconducting properties

The bulk properties of the one-layer model have been discussed previously.[12,19] We assume the sample contains identical infinitely thin superconducting layers, with c-axis repeat distance s. The Hamiltonian is taken to be $H=H_0+V$, where

$$H_0=\sum_{\mathbf{k}\sigma}\sum_{j=1}^{\infty}\xi_0(\mathbf{k})\psi^{\dagger}_{j\sigma}(\mathbf{k})\psi_{j\sigma}(\mathbf{k}) + \sum_{j\mathbf{k}\sigma}[J\psi^{\dagger}_{j\sigma}(\mathbf{k})\psi_{j+1,\sigma}(\mathbf{k})+\text{H.c.}] , \quad (1)$$

J is the quasiparticle hopping integral between adjacent layers, $\xi_0(\mathbf{k})=\mathbf{k}^2/2m_0-E_F$, $\mathbf{k}=(k_x,k_y)$, E_F is the Fermi energy, and σ is the spin index. We use units in which $\hbar=c=k_B=1$. The pair interaction term is of the BCS type given by

$$V=-\frac{1}{2}\lambda_0\sum_{j\sigma}s\int d^2\mathbf{r}\psi^{\dagger}_{j\sigma}(\mathbf{r})\psi^{\dagger}_{j,-\sigma}(\mathbf{r})\psi_{j,-\sigma}(\mathbf{r})\psi_{j\sigma}(\mathbf{r}) , \quad (2)$$

where the pair interaction strength λ_0 is restricted to energies within $\pm\omega_{\parallel}$ around E_F.

The quasiparticle Green's function matrix elements are defined in the familiar way:

$$G(k,\tau-\tau')=-\langle T[\psi_{\sigma}(k,\tau)\psi^{\dagger}_{\sigma}(k,\tau')]\rangle ,$$
$$F(k,\tau-\tau')=\langle T[\psi_{\sigma}(k,\tau)\psi_{-\sigma}(-k,\tau')]\rangle , \quad (3)$$

etc., where $k=(\mathbf{k},k_z)$, k_z is the crystal momentum in the c direction, $\langle\cdots\rangle$ denotes a thermal average, and

$$\psi_{\sigma}(k)=\Omega^{1/2}\sum_{k_z}\psi_{j\sigma}(\mathbf{k})e^{ik_z(js)} , \quad (4)$$

where Ω is the volume of the crystal. The spin index is suppressed in the Green's function matrix elements. We define the order parameter Δ by

$$\Delta=\lambda_0\sum_{k'}\langle\psi_{\sigma}(k')\psi_{-\sigma}(-k')\rangle=\frac{\lambda_0}{\beta}\sum_{k'\nu}F(k',\nu) , \quad (5)$$

where $F(k,\nu)$ is the Fourier transform of $F(k,\tau)$ in Eq. (3), and ν is the Matsubara frequency. Also, in terms of the Fourier transforms, the inverse of the Green's function matrix is

$$\hat{G}^{-1}(k,\nu)=\begin{bmatrix} i\nu-\xi_0(\mathbf{k})-2J\cos k_z s & \Delta \\ \Delta & i\nu+\xi_0(\mathbf{k})+2J\cos k_z s\end{bmatrix} , \quad (6)$$

where Δ is taken to be real. The function $2J\cos k_z s$ represents the dispersion of the tight-binding band in the c direction.

The inversion of the Green's function matrix is straightforward. Putting the results in Eq. (3), we deduce the following gap equation:

$$\Delta=\frac{\lambda_0}{\beta}\sum_{k\nu}\frac{\Delta}{\nu^2+(\epsilon_{\mathbf{k}}-2J\cos k_z s)^2+\Delta^2} , \quad (7)$$

where $\beta=1/T$, T is the temperature, and the sum on ν is subject to the constraint $|\nu|<\omega_{\parallel}$. The subsequent integration over the two-dimensional bands brings in the density of states (DOS) factor $N(0)=m_0/2\pi s$:

$$\Delta=\lambda_0 N(0)\frac{\pi}{\beta}\sum_{\nu}\frac{\Delta}{\sqrt{\nu^2+\Delta^2}} . \quad (8a)$$

It can be seen in Eq. (8a) that in this one-layer model the interlayer hopping integral J has no effect on the energy gap and the critical temperature.

The DOS in the superconducting state is given by

$$N(\omega)=\frac{1}{\pi}\sum_{k}\text{Im}G_{11}(k,\omega)|_{\nu=-i\omega+\delta} , \quad (8b)$$

where G_{11} is the first diagonal element of $\hat{G}$ and $\delta=0^+$. It is straightforward to show that

$$N(\omega)=N(0)=\frac{|\omega|}{\sqrt{\omega^2-\Delta^2}} . \quad (8c)$$

Therefore, the interlayer hopping integral also has no effect on the DOS.

B. Normal state of semi-infinite system

Before discussing the surface effects on superconductivity, it is instructive to show first how the normal-state electronic structure is solved for the semi-infinite system. We label the layers by $i=1$, 2, 3, etc. where $j=1$ is the top layer. The Green's functions are defined on a layer by layer basis:

$$G_{jj'}(\mathbf{k},\tau-\tau')=-\langle T[\psi_{j,\sigma}(\mathbf{k},\tau)\psi^{\dagger}_{j',\sigma}(\mathbf{k},\tau')]\rangle . \quad (9)$$

The equations of motion of the Green's functions can be readily written down in terms of the Fourier transforms:

$$(i\nu-\xi_0)G_{jj'}(\mathbf{k},\nu)=\delta_{jj'}+JG_{j+1,j'}(\mathbf{k},\nu) + JG_{j-1,j'}(\mathbf{k},\nu) , \quad (10)$$

for $j\neq 1$, and for $j=1$

$$(i\nu-\xi_0)G_{1j'}(\mathbf{k},\nu)=\delta_{1j'}+JG_{2j'}(\mathbf{k},\nu)\ . \tag{11}$$

Consider the special case $j'=1$. The homogeneous equations, Eq. (10), can be solved by

$$G_{j1}=A_1 e^{i(j-1)k_z s}\ , \tag{12}$$

where k_z is the solution of the equation $i\nu-\xi_0=2J\cos k_z s$. The coefficient A_1 in Eq. (12) is solved from the inhomogeneous equation, Eq. (11):

$$(i\nu-\xi_0)A_1=1+A_1 Je^{ik_z s}\ , \tag{13}$$

with the result $A_1=e^{ik_z s}/J$. Thus, we find the entire first column

$$G_{j1}=\frac{1}{J}e^{ik_z(js)}\ . \tag{14}$$

Now consider $j'=2$. One member of the equations in Eq. (10), the one with $j=1$, is inhomogeneous. The rest are solved by

$$G_{j2}=A_2 e^{i(j-2)k_z s}\ , \tag{15}$$

for $j>2$. The homogeneous member of Eq. (10) together with Eq. (11) determines both G_{12} and G_{22}, with the results,

$$G_{j2}=\frac{\sin 2k_z s}{J\sin k_z s}e^{ijk_z s}\ , \tag{16}$$

for $j\geq 2$, and

$$G_{12}=\frac{1}{J}e^{2ik_z s}\ . \tag{17}$$

The algebra becomes increasingly complex for higher values of j'. The general results are

$$G_{jj'}=\frac{\sin j'k_z s}{J\sin k_z s}e^{ik_z(js)}\ , \tag{18}$$

for $j\geq j'$, and

$$G_{jj'}=\frac{\sin jk_z s}{J\sin k_z s}e^{ik_z(j's)}\ , \tag{19}$$

for $j<j'$. This completes the task of calculating the Green's function of the semi-infinite one-layered model in the normal state.

The diagonal elements of the Green's function matrix allow us to calculate the density of states per spin state on a selected layer near the surface. For the jth layer, we have

$$N_j(\omega)=\frac{1}{\pi}\sum_{\mathbf{k}}\frac{\sin^2 jk_z s}{J\sin k_z s}\ , \tag{20a}$$

where

$$2J\cos k_z=\omega-\xi_0\ . \tag{20b}$$

The last relation, written with ξ_0 on the left-hand-side, can be readily recognized as the dispersion relation of the bulk bands, with k_z being the crystal momentum in the c-axis direction. Thus, the bulk band structure continues to influence the surface electronic structure. The integral can be carried out with the help of the transformation.

$$N_j(\omega)=\sum_{\mathbf{k}}\int_{-\pi/s}^{\pi/s}\frac{s\,dk_z}{2\pi}\sin^2(jk_z s)\delta(\omega-\xi_0-2J\cos k_z s)\ . \tag{20c}$$

The integral over $\mathbf{k}$ is easily carried out, with the result,

$$N_j(\omega)=\int_{-\pi/s}^{\pi/s}N_j(k_z)\frac{s\,dk_z}{2\pi}\ , \tag{20d}$$

where

$$N_j(k_z)=N(0)2\sin^2(jk_z s)\ . \tag{21}$$

The integral in Eq. (20d) is now trivial, with the result $N(\omega)=N(0)$ as expected. The quantity $N_j(k_z)$ defined in Eq. (21) may be regarded as the DOS in the neighborhood of k_z. It will take on added significance in systems with more than one layer per unit cell.

C. Superconductivity near the surface

In the superconducting state we need to define both the diagonal and off-diagonal Green's functions for the layers as follows:

$$\begin{aligned}G_{jj'}(\mathbf{k},\tau-\tau')&=-\langle T[\psi_{j,\sigma}(\mathbf{k},\tau)\psi^{\dagger}_{j',\sigma}(\mathbf{k},\tau')]\rangle\ ,\\ F_{jj'}(\mathbf{k},\tau-\tau')&=\langle T[\psi_{j,\sigma}(\mathbf{k},\tau)\psi_{j',-\sigma}(-\mathbf{k},\tau')]\rangle\ .\end{aligned} \tag{22}$$

The OP of the jth layer is given by

$$\Delta_j=\frac{\lambda_0}{\beta}\sum_{\mathbf{k},\nu}F_{jj}(\mathbf{k},\nu)\ , \tag{23}$$

which can be taken to be real. We define a Green's function matrix by

$$\hat{G}(\mathbf{k},\nu)=\begin{bmatrix}\hat{G}_{11}&\hat{G}_{12}&\hat{G}_{13}&\cdots\\ \hat{G}_{21}&\hat{G}_{22}&\hat{G}_{23}&\cdots\\ \cdots&\cdots&\cdots&\cdots\end{bmatrix}\ , \tag{24a}$$

where

$$\hat{G}_{jj'}=\begin{bmatrix}G_{jj'}(\mathbf{k},\nu)&F_{jj'}(\mathbf{k},\nu)\\ F^{\dagger}_{jj'}(\mathbf{k},\nu)&-G_{jj'}(\mathbf{k},-\nu)\end{bmatrix}\ . \tag{24b}$$

The inverse of the Green's function matrix has the form

$$\hat{G}^{-1}(\mathbf{k},\nu)=\begin{bmatrix}\hat{K}_{11}&\hat{K}_{21}&0&0&0&\cdots\\ \hat{K}_{12}&\hat{K}_{22}&\hat{K}_{32}&0&0&\cdots\\ 0&\hat{K}_{23}&\hat{K}_{33}&\hat{K}_{43}&0&\cdots\\ 0&0&\hat{K}_{34}&\hat{K}_{44}&\hat{K}_{54}&\cdots\\ \cdots&\cdots&\cdots&\cdots&\cdots&\cdots\end{bmatrix}\ , \tag{25a}$$

where the $\hat{K}_{jj'}$ are 2×2 matrices defined by

$$\hat{K}_{jj}=\begin{bmatrix} i\nu-\xi_0(\mathbf{k}) & \Delta_j \\ \Delta_j & i\nu+\xi_0(\mathbf{k}) \end{bmatrix}, \tag{25b}$$

and

$$\hat{K}_{j,j+1}=\hat{K}^T_{j+1,j}=\begin{bmatrix} -J & 0 \\ 0 & J \end{bmatrix}. \tag{25c}$$

In the bulk system the OP depends only on the density of states and the pair interaction in the plane, but not on the hopping integral J. We will now show that in a semi-infinite system the OP is independent of the layer index because it is also unaffected by hopping. We do so by invoking the ansatz $\Delta_j=\Delta$ for all j and verifying that this is consistent with the set of gap equations, Eq. (23).

As a first step toward solving the gap equation, we introduce a shorthand symbol

$$\hat{G}_{jj'}=\begin{bmatrix} G_{jj'} & F_{jj'} \\ \bar{F}_{jj'} & \bar{G}_{jj'} \end{bmatrix}, \tag{26}$$

for the matrix elements in Eq. (24b), and $\hat{1}$ is a semi-infinite unit matrix. We then write the matrix identity $\hat{G}^{-1}\hat{G}=\hat{1}$ in the component form. For $j\neq 1$, we find

$$(i\nu-\xi_0)G_{jj'}+\Delta\bar{F}_{jj'}-JG_{j+1,j'}-JG_{j-1,j'}=\delta_{jj'}, \tag{27a}$$

$$\Delta G_{jj'}+(i\nu+\xi_0)\bar{F}_{jj'}+J\bar{F}_{j+1,j'}+J\bar{F}_{j-1,j'}=0, \tag{27b}$$

and two more similar equations, and for $j=1$

$$(i\nu-\xi_0)G_{1j'}+\Delta\bar{F}_{1j'}-JG_{2j'}=\delta_{1j'}, \tag{27c}$$

$$\Delta G_{1j'}+(i\nu+\xi_0)\bar{F}_{1j'}+J\bar{F}_{2j'}=0, \tag{27d}$$

and two more similar equations. These equations are solved by the same method as the normal-state case. Considering $j'=1$, the linear equations in Eqs. (27a) and (27b) are homogeneous and are solved by

$$G_{j1}=\frac{1}{\Delta}[(i\nu+\xi_0+2J\cos k_+ s)A_+e^{ik_+(js)} +(i\nu+\xi_0+2J\cos k_- s)A_-e^{ik_-(js)}], \tag{28a}$$

$$\bar{F}_{j1}=A_+e^{ik_+(js)}+A_-e^{ik_-(js)}, \tag{28b}$$

where

$$2J\cos k_\pm s=-\xi_0\pm i\sqrt{\nu^2+\Delta^2}. \tag{29a}$$

The coefficients $A_\pm$ are to be determined by Eqs. (27c) and (27d), with the results

$$A_\pm=\frac{\mp\Delta}{2iJ\sqrt{\nu^2+\Delta^2}}. \tag{29b}$$

The gap equation, Eq. (23), now has the form

$$\Delta=-\frac{\lambda_0 N(0)}{\beta}\sum_\nu\int_{-\infty}^{\infty}\frac{\Delta d\xi_0}{2iJs\sqrt{\nu^2+\Delta^2}}[e^{ik_+s}-e^{ik_-s}]. \tag{30}$$

In the next step we reduce the gap equation to a more familiar form by a series of transformations. First we transform from the sum over Matsubara frequencies to an integral over real frequencies ω. Then we write

$$e^{ik_\pm s}=\int_{-\pi/s}^{\pi/s}2J\sin(k_z s)e^{ik_z s}\delta(2J\cos k_z s+\xi_0\mp\sqrt{\omega^2-\Delta^2})s\,dk_z =\frac{1}{\pi}\int_{-\pi/s}^{\pi/s}2J\sin(k_z s)e^{ik_z s}\,\mathrm{Im}\frac{s\,dk_z}{2J\cos k_z s+\xi_0\mp\sqrt{\omega^2-\Delta^2}}. \tag{31}$$

The step of taking the imaginary part may be simply replaced by a factor $-i$ because the real part vanishes upon integration over ξ_0. Putting the final result into Eq. (30), transforming back into Matsubara frequencies, and integrating over ξ_0, we obtain the gap equation[20]

$$\Delta=\frac{\lambda_0}{\beta}\sum_\nu\int_{-\pi/s}^{\pi/s}\frac{N_1(k_z)\Delta}{\sqrt{\nu^2+\Delta^2}}\frac{s\,dk_z}{2\pi}, \tag{32}$$

where $N_1(k_z)$ has been defined in Eq. (21). The k_z integral is readily carried out, and the resulting gap equation is identical to Eq. (8). This confirms that the top layer has the same gap as the bulk.

The same calculation can be carried out for the jth layer. The gap equation is found to be similar to Eq. (32) except that the k_z integral has the integrand $N_j(k_z)$. The result of the k_z integral is independent of the layer index j, which justifies the ansatz that all layers have the same gap Δ for the bulk superconductor.

The DOS $N_j(\omega)$ in the superconducting state is calculated from the diagonal elements G_{jj}. The same set of transformations we have used to reduce the gap equation helps to reduce the algebra. The final answer, after carrying out the $\mathbf{k}$ or ξ_0 integration, is

$$N_j(\omega)=\frac{|\omega|}{\sqrt{\omega^2-\Delta^2}}\int_{-\pi/s}^{\pi/s}N_j(k_z)\frac{s\,dk_z}{2\pi}. \tag{33}$$

Again, the k_z integral is independent of the layer index j, which implies that all layers have the same DOS as the bulk superconductor.

III. THE TWO-LAYER MODEL

The two-layer model consists of two conducting layers, one superconducting (S) and one normal (N), in a unit cell. For simplicity, the two layers are assumed to have identical two-dimensional quasiparticle band structures. In addition, the quasiparticles in the S layer can hop into the N layer in the same unit cell with the hopping integral J_1, and into the N layer in the neighboring unit cell with J_2. In YBCO there are three conducting layers per unit cell. The two-layer model depicts the two CuO_2 layers as one S layer and the CuO chain layer as an N layer.

In BSCCO the two CuO_2 layers are assumed to act like one S layer while the BiO double layers comprise one N layer. The unit cell doubling is neglected. The model, shown schematically in Fig. 1, is an extension to $J_1 \neq J_2$ of the S-N model studied by Abrikosov.[21] We find this generalization of the hopping integrals necessary in order to model the more complex energy band and Fermi-surface geometry of the real materials. This section is organized parallel to Sec. II for the one-layer model. We will discuss in three subsections the superconducting state of the infinite solid, the normal state of the semi-infinite solid, and last the superconducting state of the semi-infinite solid.

A. Bulk superconducting properties

The model Hamiltonian is a straightforward generalization of Eqs. (1) and (2). We write $H = H_0 + V$, where the band energy term is

$$H_0 = \sum_{\mathbf{k}\sigma} \sum_{j=1}^{\infty} \sum_{n=1}^{2} \xi_0(\mathbf{k}) \psi^\dagger_{jn\sigma}(\mathbf{k}) \psi_{jn\sigma}(\mathbf{k}) + \sum_{jk\sigma} [J_1 \psi^\dagger_{j1\sigma}(\mathbf{k}) \psi_{j2\sigma}(\mathbf{k}) + J_2 \psi^\dagger_{j2\sigma}(\mathbf{k}) \psi_{j+1,1\sigma}(\mathbf{k}) + \text{H.c.}] , \quad (34)$$

where $n = 1,2$ is the layer index within a unit cell. The interaction term is present only in the S layer, which is labeled by 1:

$$V = -\frac{1}{2} \sum_{j\sigma} \sum_{\mathbf{k}\mathbf{k}'} \lambda_0 \psi^\dagger_{j1\sigma}(\mathbf{k}) \psi^\dagger_{j1,-\sigma}(-\mathbf{k}) \times \psi_{j1,-\sigma}(-\mathbf{k}') \psi_{j1\sigma}(\mathbf{k}') , \quad (35)$$

where only the S layers have the pair coupling strength λ_0, which is cut off at energies differing from E_F by $\omega_\parallel$. The interaction V leads to s-wave intralayer pairing, although the main effect under discussion is independent of the pairing symmetry.

The bulk properties of this model have been discussed elsewhere.[12-14] A brief summary will be given here for completeness. The quasiparticle Green's function matrix elements are defined as in Eq. (3) for the one-layer case:

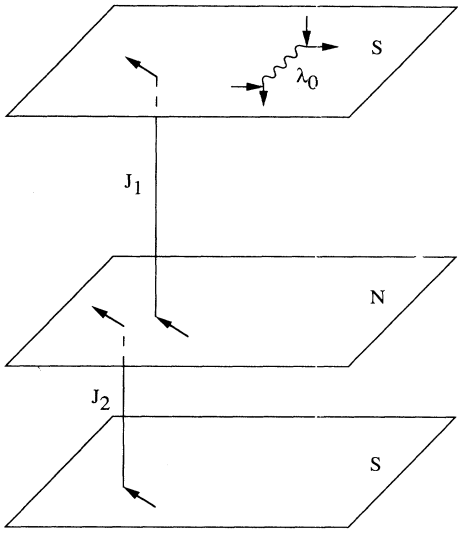

FIG. 1. A schematic drawing of the two-layer model under consideration.

$$G_{nn'}(k,\tau-\tau') = -\langle T[\psi_{n\sigma}(k,\tau)\psi^\dagger_{n'\sigma}(k,\tau')]\rangle ,$$
$$F_{nn'}(k,\tau-\tau') = \langle T[\psi_{n\sigma}(k,\tau)\psi_{n',-\sigma}(-k,\tau')]\rangle , \quad (36)$$

where

$$\psi_{n\sigma}(k) = \Omega^{1/2} \sum_{k_z} \psi_{jn\sigma}(\mathbf{k}) e^{ik_z[js+(n-1)d]} . \quad (37)$$

In the above equation s is the thickness of the unit cell in the c direction, and d is the separation between layer 1 and layer 2 within the same cell. The separation between adjacent layers in adjacent cells will be denoted by $d' = s - d$. The spin index is suppressed in the Green's function matrix elements. We define the order parameter Δ for the S layers by

$$\Delta = \lambda_0 \sum_{k'} \langle \psi_{1\sigma}(k')\psi_{1,-\sigma}(-k')\rangle = \frac{\lambda_0}{\beta} \sum_{k'\nu} F_{11}(k',\nu) . \quad (38)$$

The inverse of the Green's function matrix has the form

$$\hat{G}^{-1}(k,\nu) = \begin{bmatrix} i\nu-\xi_0(\mathbf{k}) & -g(k_z) & \Delta & 0 \\ -g^*(k_z) & i\nu-\xi_0(\mathbf{k}) & 0 & 0 \\ \Delta^* & 0 & i\nu+\xi_0(\mathbf{k}) & g(k_z) \\ 0 & 0 & g^*(k_z) & i\nu+\xi_0(\mathbf{k}) \end{bmatrix} , \quad (39)$$

where the quantity

$$g(k_z) = J_1 e^{ik_z d} + J_2 e^{-ik_z d'} \equiv \epsilon_\perp(k_z) e^{-i\phi(k_z)} , \quad (40)$$

with

$$\epsilon_\perp(k_z) = [J_1^2 + J_2^2 + 2J_1 J_2 \cos k_z s]^{1/2} , \quad (41)$$

$$\tan[\phi(k_z)] = \frac{J_2 \sin k_z d' - J_1 \sin k_z d}{J_2 \cos k_z d' + J_1 \cos k_z d} . \quad (42)$$

The functions $\pm\epsilon_\perp(k_z)$ represent the dispersions of the two tight-binding bands in the c direction.

The inversion of the Green's function matrix is

straightforward. Putting the results in Eq. (38), we deduce the following gap equation:

$$\Delta=\frac{\lambda_0}{\beta}\sum_{k\nu}\frac{[\nu^2+\xi_0^2(\mathbf{k})]\Delta}{D}\ , \tag{43}$$

where the sum on the Matsubara frequencies ν is under the constraint that $|\nu|<\omega_\parallel$. The quantity D is the determinant of the inverse Green's function matrix:

$$D=(\nu^2+\xi_0^2)^2+2\epsilon_\perp^2(\nu^2-\xi_0^2)+\epsilon_\perp^4+\Delta^2(\nu^2+\xi_0^2)\ . \tag{44}$$

We will choose the OP to be real. The subsequent integration over the two-dimensional bands brings in the DOS factor $N(0)=m_0/2\pi s$, but $\epsilon_\perp(k_z)$ remains explicitly in the gap equation. Consequently, the c-axis dispersion of the quasiparticle bands enters the superconducting properties in a number of ways to be discussed later.

The critical temperature T_c is solved from the linearized version of Eq. (43), which is

$$1=\tfrac{1}{2}\lambda_0 N(0)\int_0^{\omega_\parallel}\tanh\frac{\beta_c\omega}{2}d\omega \times\int_{-\pi/s}^{\pi/s}\frac{s\,dk_z}{2\pi}\left[\frac{1}{\omega}+\frac{\omega}{\omega^2-\epsilon_\perp^2(k_z)}\right], \tag{45}$$

where $\beta_c=1/T_c$. It is seen that the c-axis band dispersion enters the T_c equation as a pair breaker. This effect has been discussed previously by the present authors for a general two-layer model.[12–14] In the limit of zero hopping the critical temperature is solved from

$$\lambda_0 N(0)a_\parallel(T_{c0})=1\ , \tag{46}$$

where $a_\parallel(T)=\ln(2\gamma\omega_\parallel/\pi T)$, and $\gamma=1.78$. We use T_{c0} to set the energy scale in our numerical analysis. With increasing hopping, T_c is lowered steadily from the zero hopping limit T_{c0}. In the limit of strong hopping, i.e., $J_1,J_2\gg\omega_\parallel$, the critical temperature is solved from

$$\tfrac{1}{2}\lambda_0 N(0)a_\parallel(T_{c\infty})=1\ . \tag{47}$$

It can be seen that $T_{c\infty}<T_{c0}$. In the intermediate hopping regime, T_c falls monotonically with increasing J's for a fixed ratio of J_1/J_2.

The OP Δ at zero temperature depends also on the hopping strengths. In the zero hopping limit, Eq. (45) reduces to the BCS gap equation for the S layer alone. Similar to T_c, Δ decreases steadily with increasing hopping. In the infinite hopping limit, the OP corresponds to that of a BCS superconductor with the pair coupling constant equal to $\frac{1}{2}\lambda_0$.[22] The temperature dependence of the OP, $\Delta(T)$, has the typical BCS behavior.[12–14]

The DOS curves in the superconducting state for the two kinds of layers are calculated in the same way as the one-layer case:

$$N_n(\omega)=\frac{1}{\pi}\sum_{kn}\mathrm{Im}G_{nn}(k,\nu)|_{\nu\to-i\omega+\delta}\ , \tag{48}$$

where $n=1$ or 2, and $\delta=0^+$. The details of this calculation are in Ref. 13. In Fig. 2 we show $N_1(\omega)$ for the S layer in the top panel and $N_2(\omega)$ for the N layer in the bottom panel for the set of model parameters $J_1/T_{c0}=0.5$ and $J_2/T_{c0}=1$. Shown in Fig. 3 is the total DOS $N_s(\omega)=N_1(\omega)+N_2(\omega)$. All three curves have the double peak structure observed in many layered superconductors, including YBCO,[8] BSCCO,[4] and the layered organic superconductor κ-(BEDT-TTF)$_2$Cu(NCS)$_2$ which has $T_c=11$ K.[23] The structure originates from two types of pairing states, intraband pairing, which gives rise to the inner peaks, and interband pairing which gives the outer peaks. The relative weights of the two sets of peaks are different in different layers. The S layer shows stronger interband peaks, while the N layer has stronger intraband peaks. The significance of this result will be discussed further in connection with tunneling experiments. The DOS curves in all cases vanish inside the threshold values $\pm\omega_-''$, where

$$\omega_-''=\tfrac{1}{2}[\sqrt{4(J_1-J_2)^2+\Delta^2}-\Delta]\ . \tag{49}$$

The system is gapless if $J_1=J_2$. The intraband pairing peaks appear at $\pm\omega_0'$ where

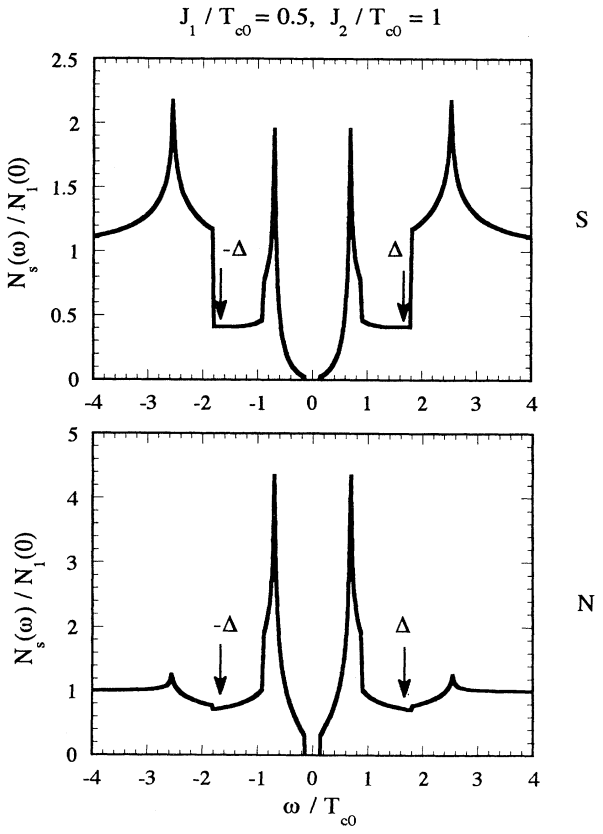

FIG. 2. The density of states curves in the superconducting state for the S layer and the N layer of the two-layer model in Fig. 1. The model parameters are $J_1/T_{c0}=0.5$, $J_2/T_{c0}=1$, and $\lambda_0 N(0)=0.5$. The quantity T_{c0} is the critical temperature when all interlayer hoppings are turned off, as defined in Eq. (46).

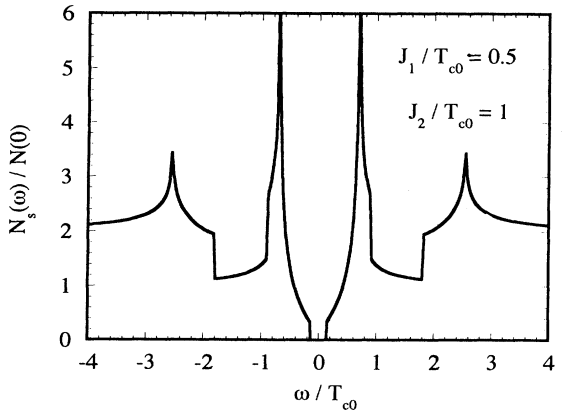

FIG. 3. The total bulk DOS for the two-layer model in Fig. 1.

$$\omega_0'=\frac{\Delta}{2}\left[1-\frac{\Delta^2}{4(J_1+J_2)^2}\right]^{1/2} . \tag{50}$$

The interband pairing peaks occur at $\pm\omega_+'$, where

$$\omega_+'=\tfrac{1}{2}[\sqrt{4(J_1+J_2)^2+\Delta^2}+\Delta] . \tag{51}$$

Both sets of peaks are logarithmic singularities.

Another way to understand the multiple peak structure can be obtained from an analysis of the quasiparticle band structure. Consider the determinant D of the inverse Green's function in Eq. (44). After replacing the Matsubara frequency ν by $i\omega$, where ω is the real frequency, the quartic equation $D(\omega)=0$ gives four branches of quasiparticle bands with energies

$$\omega^2(k)=\xi_0^2(\mathbf{k})+\epsilon_1^2(k_z)+\tfrac{1}{2}\Delta^2\pm R(k) , \tag{52}$$

where

$$R^2(k)=[\xi_0^2(\mathbf{k})+\Delta^2]\epsilon_1^2(k_z)+\tfrac{1}{4}\Delta^4 . \tag{53}$$

Two of the bands with $\omega>0$ are above the Fermi energy, and two bands with $\omega<0$ are below the Fermi energy. Consider the two bands above the Fermi energy. The bottom of the lower band, "−" sign in Eq. (52), corresponds to the threshold of the DOS curve, ω_-'' in Eq. (49), while the top of the lower band determines the position of the inner peak, ω_0' in Eq. (50). The bottom of the upper band, "+" sign in Eq. (52), is the position of the interband pairing peak, ω_+' in Eq. (51). For the chosen set of parameters, the top of the upper band is outside the energy range of interest. Thus, the DOS of multilayer superconductors is intrinsically complex because it exhibits Van Hove-like singularities of the quasiparticle bands. The logarithmic behavior of the peaks results from the quasiparticle band dispersion along the c axis. It is not appropriate to interpret the structure of the DOS as evidence of multiple gaps or gap anisotropy. In this connection, it should be noted that the quantity 2Δ at zero temperature is equal to $3.5T_c$ in a weak-coupling theory. The quantity $2\omega_+'$, which has been identified in junction tunneling experiments as the gap feature, is always greater than $3.5T_c$, while $2\omega_0'$, which has been called the inner gap feature, is always less than $3.5T_c$.[6,8]

We have chosen the hopping parameters J_1 and J_2 to be in the range where the double-peak structure of the DOS is clearly demonstrated, even exaggerated compared with experiments. The structure disappears in the extreme band limit, $J_1,J_2\gg T_c$, as shown by the present authors in Ref. 22. While it should be possible to extract the hopping strengths from a band calculation, there are two practical difficulties in making a convincing estimate this way. These are the following: (1) Both YBCO and BSCCO have more than two layers in a unit cell, and it is not clear how to simulate them realistically with a two-layer model; and (2) the band splittings of real materials vary in the k_x,k_y plane so that all hopping parameters are $\mathbf{k}$ dependent. The values we have chosen are intermediate between the strongest and the weakest hoppings in the two-dimensional Brillouin zone.[24] In addition, we have shown in Ref. 16 that the hopping parameters needed to fit the penetration depth of YBCO fall in the same energy range. These parameters are $J_1/T_{c0}=3.0$, $J_2/T_{c0}=2.6$, and $\beta=5$, where β is the ratio of the quasiparticle effective masses of S and N layers. Bear in mind that we have used an oversimplified model in which the energy band of the normal chain layer is approximated by an isotropic free particle band. A more realistic calculation, which treats the normal layer as tight-binding chains, would require larger hopping parameters, closer to those found in band calculations. Due to all of these limitations imposed by the two-layer model, we do not expect the same set of parameters to fit both DOS and penetration depth results. Nonetheless, the fact that they do agree in order of magnitude gives us confidence that our discussion of the DOS structure is realistic.

B. Normal state of semi-infinite system

The formulation of the semi-infinite problem follows the same steps as the one-layer system. We define

$$G_{jn,j'n'}(k,\tau-\tau')=-\langle T[\psi_{jn,\sigma}(\mathbf{k},\tau)\psi_{j'n',\sigma}^{\dagger}(\mathbf{k},\tau')]\rangle , \tag{54}$$

where $n=1$ is an S layer. The equations of motion of the normal state ($\Delta=0$) Green's functions are, in terms of the Fourier transforms,

$$(i\nu-\xi_0)G_{j1,j'n'}(\mathbf{k},\nu)=\delta_{jj'}\delta_{1n'}+J_1G_{j2,j'n'}(\mathbf{k},\nu)+J_2G_{j-1,2,j'n'}(\mathbf{k},\nu) , \tag{55}$$

and

$$(i\nu-\xi_0)G_{j2,j'n'}(\mathbf{k},\nu)=\delta_{jj'}\delta_{2n'}+J_1G_{j1,j'n'}(\mathbf{k},\nu)+J_2G_{j+1,1,j'n'}(\mathbf{k},\nu) , \tag{56}$$

for $j\neq1$. For $j=1$

$$(i\nu-\xi_0)G_{11,j'n'}(\mathbf{k},\nu)=\delta_{1j'}\delta_{1n'}+JG_{12,j'n'}(\mathbf{k},\nu) ,$$

and

$$(i\nu-\xi_0)G_{12,j'n'}(\mathbf{k},\nu)=\delta_{1j'}\delta_{2n'}+J_1G_{11,j'n'}(\mathbf{k},\nu)+J_2G_{21,j'n'}(\mathbf{k},\nu) . \tag{57}$$

Consider $j'=1$ and $n'=1$. The homogeneous equations, Eqs. (55) and (56), are solved by

$$G_{jn,11}=A_n e^{ik_z[(j-1)s+d(n-1)]}, \tag{58}$$

where

$$(i\nu-\xi_0)^2=J_1^2+J_2^2+2J_1J_2\cos k_z s\equiv\epsilon_\perp^2(k_z). \tag{59}$$

The quantity $\epsilon_\perp(k_z)$ was defined in Eq. (41). The coefficients A_n satisfy

$$A_2=A_1 e^{i\phi(k_z)},$$

where $\phi(k_z)$ was defined in Eq. (42). The inhomogeneous equation, the top equation in Eq. (57), allows a complete determination of the coefficients A_n. To avoid repetition, we will only present the results of the calculation:

$$G_{11,11}=\frac{J_1 e^{ik_z s}+J_2}{J_2\epsilon_\perp(k_z)}, \tag{60}$$

and

$$G_{12,11}=\frac{1}{J_2}e^{ik_z s}. \tag{61}$$

All other members of $G_{jn,11}$ can be written down according to the formula in Eq. (58). Similarly, for $j'=1,n'=2$ we find

$$G_{12,12}=\frac{\epsilon_\perp(k_z)}{J_1J_2}e^{ik_z s}, \tag{62}$$

and

$$G_{11,12}=G_{12,11}.$$

For later purposes, we need to write down the general diagonal elements. These are

$$G_{j1,j1}=\frac{J_1 e^{ik_z s}+J_2}{J_1J_2\sin k_z s\,\epsilon_\perp(k_z)}\times[J_1\sin jk_z s+J_2\sin(j-1)k_z s]e^{i(j-1)k_z s}, \tag{63}$$

and

$$G_{j2,j2}=\frac{\epsilon_\perp(k_z)\sin jk_z s}{J_1J_2\sin k_z s}e^{ijk_z s}. \tag{64}$$

The density of states in the layers are calculated like the one-layer case. We employ the same procedure which led from Eq. (20a) to Eq. (20d) to transform the result into

$$N_{jn}(\omega)=\int_{-\pi/s}^{\pi/s}N_{jn}(k_z)\frac{s\,dk_z}{2\pi}, \tag{65}$$

where

$$N_{j1}(k_z)=N(0)\frac{2[J_1\sin jk_z s+J_2\sin(j-1)k_z s]^2}{\epsilon_\perp^2(k_z)}, \tag{66}$$

and

$$N_{j2}(k_z)=N(0)2\sin^2(jk_z s). \tag{67}$$

The relation between the energy ω and the c-axis momentum k_z is

$$(\omega-\xi_0)^2=\epsilon_\perp^2(k_z). \tag{68}$$

It is interesting to work out the integral in Eq. (65) for a few specific values of j. For instance,

$$N_{11}(\omega)=N(0)\int_{-\pi/s}^{\pi/s}\frac{2J_1^2\sin^2k_z s}{J_1^2+J_2^2+2J_1J_2\cos k_z s}\frac{s\,dk_z}{2\pi}. \tag{69}$$

The result of the integral is 1 if $J_1>J_2$ and J_1^2/J_2^2 if $J_1<J_2$. This indicates that in the latter case, some electron states are missing. A close examination reveals that, under the condition $J_1<J_2$, a band of surface states is formed with $k_z s=\pi+i\kappa$, where $\kappa=\ln(J_2/J_1)$.[25] This surface band has $\epsilon_\perp(k_z)=0$. Recall that the quasiparticle band energies in the infinite system are given by $\xi_0(\mathbf{k})\pm\epsilon_\perp(k_z)$, and the Fermi surfaces form two corrugated cylindrical sheets. Thus the surface band intersects the Fermi energy on a circular cylinder in the middle of the two sheets. They contribute to $N_{11}(k_z)$ as a δ function at $\epsilon_\perp(k_z)=0$ with the weight $1-r^2$, where $r=J_1/J_2$. Similarly, in the S layer of the jth cell the weight of the surface band is $(r)^{-2j}(r^2-1)$. On the other hand, the integral in N_{j2} is always equal to 1. This means that the surface states have no weight in all N layers of the system. The wave function of the surface band is sketched in Fig. 4. The surface states do not form under the opposite condition, i.e., $J_1\geq J_2$. We will show that the existence of this surface band has a strong influence on the superconducting properties near the surface.

It is worth emphasizing here that the complex wave vector k_z and the wave function of the surface state are entirely determined by the bulk band structure. In real materials the surface may undergo relaxation and/or reconstruction so that the hopping parameters near the top layer may be modified from those of the bulk. In this event, only the relative weight of the surface state versus the bulk state would be changed. As long as $J_1<J_2$ near the top layer, the surface state exists and its physical properties, such as its decay length and its vanishing

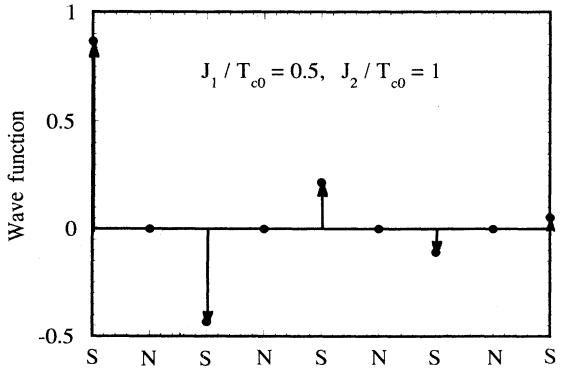

FIG. 4. The wave function of the surface band for the model in Fig. 1 with $J_1/J_2=0.5$, plotted versus the layer index. The wave function vanishes on all normal layers.

weight on even layers, remain intact. We will return to this point in our discussion of three- and four-layer models.

C. Superconductivity near the surface

The quasiparticle Green's function matrix elements are defined in the familiar way:

$$G_{jn,j'n'}(\mathbf{k},\tau-\tau')=-\langle T[\psi_{jn\sigma}(\mathbf{k},\tau)\psi^{\dagger}_{j',n'\sigma}(\mathbf{k},\tau')]\rangle ,$$
$$F_{jn,j'n'}(\mathbf{k},\tau-\tau')=\langle T[\psi_{jn\sigma}(\mathbf{k},\tau)\psi_{j'n',-\sigma}(-\mathbf{k},\tau')]\rangle , \tag{70}$$

where the spin indices are suppressed. The indices j and n label the unit cells and layers within each cell respectively, $n=1$ being the S layer and $n=2$ the N layer. We define the jth S layer order parameter Δ_j by

$$\Delta_j=\frac{\lambda_0}{\beta}\sum_{\mathbf{k}\nu}F_{j1,j1}(\mathbf{k},\nu) , \tag{71}$$

which can be taken as real. The inverse of the Green's function matrix has the form

$$\hat{G}^{-1}(\mathbf{k},\nu)=\begin{bmatrix} \hat{K}_{11} & \hat{K}_{21} & 0 & 0 & 0 & \cdots \\ \hat{K}_{12} & \hat{K}_{22} & \hat{K}_{32} & 0 & 0 & \cdots \\ 0 & \hat{K}_{23} & \hat{K}_{33} & \hat{K}_{43} & 0 & \cdots \\ 0 & 0 & \hat{K}_{34} & \hat{K}_{44} & \hat{K}_{54} & \cdots \\ \cdots & \cdots & \cdots & \cdots & \cdots & \cdots \end{bmatrix} , \tag{72}$$

where the $\hat{K}_{jj'}$ Are 4×4 matrices defined by

$$\hat{K}_{jj}=\begin{bmatrix} i\nu-\xi_0(\mathbf{k}) & -J_1 & \Delta_j & 0 \\ -J_1 & i\nu-\xi_0(\mathbf{k}) & 0 & 0 \\ \Delta_j & 0 & i\nu+\xi_0(\mathbf{k}) & J_1 \\ 0 & 0 & J_1 & i\nu+\xi_0(\mathbf{k}) \end{bmatrix} \tag{73}$$

and

$$\hat{K}_{j,j+1}=\hat{K}^{T}_{j+1,j}=\begin{bmatrix} 0 & -J_2 & 0 & 0 \\ 0 & 0 & 0 & 0 \\ 0 & 0 & 0 & J_2 \\ 0 & 0 & 0 & 0 \end{bmatrix} . \tag{74}$$

The evaluation of the Green's function matrix elements follows the same procedure as that for the one-layer system. We define a Green's function matrix by Eq. (24a) except that every matrix element $\hat{G}_{jj'}$ is a 4×4 matrix of the form

$$\hat{G}_{jj'}=\begin{bmatrix} G_{j1,j'1} & G_{j1,j'2} & F_{j1,j'1} & F_{j1,j'2} \\ G_{j2,j'1} & G_{j2,j'2} & F_{j2,j'1} & F_{j2,j'2} \\ \bar{F}_{j1,j'1} & \bar{F}_{j1,j'2} & \bar{G}_{j1,j'1} & \bar{G}_{j1,j'2} \\ \bar{F}_{j2,j'1} & \bar{F}_{j2,j'2} & \bar{G}_{j2,j'1} & \bar{G}_{j2,j'2} \end{bmatrix} , \tag{75}$$

where, as for the one-layer problem in the last section, $\bar{F}_{jn,j'n'}(\mathbf{k},\nu)=F^{\dagger}_{jn,j'n'}(\mathbf{k},\nu)$ and $\bar{G}_{jn,j'n'}(\mathbf{k},\nu)=-G_{jn,j'n'}(\mathbf{k},-\nu)$. The matrix identity $\hat{G}^{-1}\hat{G}=\hat{1}$, when expanded into components yields the following set of equations for the Green's functions:

$$\begin{aligned} &(i\nu-\xi_0)G_{j1,j'n'}+\Delta_j\bar{F}_{j1,j'n'}-J_1G_{j2,j'n'}-J_2G_{j-1,2,j'n'}=\delta_{jj'}\delta_{1n'} , \\ &\Delta_jG_{j1,j'n'}+(i\nu+\xi_0)\bar{F}_{j1,j'n'}+J_1\bar{F}_{j2,j'n'}+J_2\bar{F}_{j-1,2,j'n'}=0 , \\ &(i\nu-\xi_0)G_{j2,j'n'}-J_1G_{j1,j'n'}-J_2G_{j+1,1,j'n'}=\delta_{jj'}\delta_{2n'} , \\ &(i\nu+\xi_0)\bar{F}_{j2,j'n'}+J_1\bar{F}_{j1,j'n'}+J_2\bar{F}_{j+1,1,j'n'}=0 , \end{aligned} \tag{76}$$

for $j\neq1$ and for $j=n=1$

$$\begin{aligned} &(i\nu-\xi_0)G_{11,j'n'}+\Delta_1\bar{F}_{11,j'n'}-J_1G_{12,j'n'}=\delta_{1j'}\delta_{1n'} , \\ &\Delta_1G_{11,j'n'}+(i\nu+\xi_0)\bar{F}_{11,j'n'}+J_1\bar{F}_{12,j'n'}=0 . \end{aligned} \tag{77}$$

The matrix inversion problem in the superconducting state is hampered by the fact that the Δ_j's are expected to vary with j. To render the calculation tractable, we make a local approximation such that we approximate all OP's by Δ_j in deriving the gap equation for the jth cell. The rationale of this procedure is that the OP of each layer is affected mainly by the electronic structure of that layer and less so by the two adjacent N layers. The approximation treats the immediate environment of the S layer exactly, while the much reduced effects of the more distant S layers are handled approximately.

We summarize very briefly the algebraic procedure for solving the equations for the Green's functions. Consider the case $j'=n'=1$. We replace Δ_j in the homogeneous equations in Eq. (76) by Δ_1. The equations are then cast into a matrix diagonalization problem, with the following eigenvectors:

$$\begin{aligned} G_{jn,11}&=g_{n+}e^{i(j-1)k_+s}+g_{n-}e^{i(j-1)k_-s} , \\ \bar{F}_{jn,11}&=f_{n+}e^{i(j-1)k_+s}+f_{n-}e^{i(j-1)k_-s} , \end{aligned} \tag{78}$$

where $k_{\pm}$ satisfy the equations

$$\epsilon_1^2(k_{\pm})=\xi_0^2-\nu^2\pm2i[\nu^2\xi_0^2+\tfrac{1}{4}\Delta_1^2(\xi_0^2+\nu^2)]^{1/2} . \tag{79}$$

The coefficients g and f are determined within a common factor from Eq. (76), and are completely determined by the inhomogeneous equations in Eq. (77). The important ones are

$$\begin{aligned} g_{1\pm}&=\frac{\mp(i\nu-\xi_0)e^{ik_{\pm}s}}{\bar{D}_{\pm}}[(i\nu+\xi_0)^2-\epsilon_1^2(k_{\pm})] , \\ f_{1\pm}&=\frac{\mp\Delta_1e^{ik_{\pm}s}}{\bar{D}_{\pm}}[\nu^2+\xi_0^2] , \end{aligned} \tag{80}$$

where

$$\bar{D}_{\pm}=4iJ_2(J_1+J_2e^{ik_{\pm}s})[\nu^2\xi_0^2+\tfrac{1}{4}\Delta_1^2(\xi_0^2+\nu^2)]^{1/2} . \tag{81}$$

We use these results to set up the gap equation for Δ_1 and calculate the DOS for the top layer. Similarly, by approximating all Δ's by Δ_j, we determine $G_{j1,j1}$ and $F_{j1,j1}$ for the S layer of the jth unit cell.

A generalization of the integral transformation introduced in Eq. (31) allows a significant simplification of the results. The gap equation for the jth layer is

$$\Delta_j=\lambda_0\int_0^{\omega_\parallel}\tanh\frac{\omega}{2T}d\omega\int_{-\infty}^{\infty}d\xi_0\int_{-\pi/s}^{\pi/s}\frac{s\,dk_z}{2\pi}N_{j1}(k_z)\times\frac{[\omega^2-\xi_0^2]\Delta_j}{D_j}\ , \tag{82}$$

where, in analogy with Eq. (81),

$$D_j=(\omega^2-\xi_0^2)^2-2\epsilon_1^2(\omega^2+\xi_0^2)+\epsilon_1^4-\Delta_j^2(\omega^2-\xi_0^2)\ , \tag{83}$$

and $N_{j1}(k_z)$ is the normal-state DOS of the S layer in the jth unit cell in the neighborhood of k_z defined in Eq. (66). Recall that, in case $J_1<J_2$, a surface state exists in the band gap and $N_{j1}(k_z)$ has a δ function term at $k_z s=\pi+i\kappa$. This gives rise to an additional term on the right-hand side of Eq. (82), namely,

$$\lambda_0\int_0^{\omega_\parallel}\tanh\frac{\omega}{2T}d\omega\int_{-\infty}^{\infty}d\xi_0\int_{-\pi/s}^{\pi/s}\frac{s\,dk_z}{2\pi}\times r^{-2j}(r^2-1)\times\frac{\Delta_j}{\omega^2-\xi_0^2-\Delta_j^2}\ , \tag{84}$$

where $r=J_1/J_2$. The added term in Eq. (84) does not contain the pair breaker ϵ_1 in the T_c equation for the bulk, Eq. (45). The reason for this is that the surface state has no weight in the normal layer, with the result that its contribution to superconductivity is not diluted by the normal layers. This causes the gap Δ_j near the surface to be higher than that of the bulk.

The integral over ξ_0 in Eq. (82) can be performed analytically. The resulting gap equations have been solved at $T=0$ and the results are shown in Fig. 5 for a range of J's while holding $J_1/J_2=0.5$. The top S layer OP, denoted by Δ_1, is significantly larger than the bulk OP Δ when the hopping strengths are comparable to T_c.

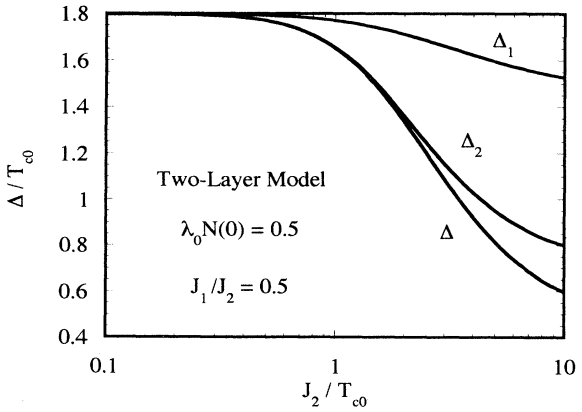

FIG. 5. The OP of the top two S layers Δ_1 and Δ_2 and that of the bulk Δ for the two-layer model in Fig. 1 plotted as functions of J_2 for a fixed ratio $J_1/J_2=0.5$.

The OP Δ_2 of the S layer in the next cell is not very different from Δ. Beyond the second unit cell, the surface effect is negligible. The fact that Δ_1 is larger than Δ is consistent with the top layer having a higher transition temperature T_{c1} than the bulk T_c, a result which we obtain from Eqs. (82) and (84) without the local approximation. This effect has negligible consequences in bulk measurements on bulk samples, but may affect results on thin samples or surface-sensitive measurements on bulk materials.

The DOS of the nth layer in the jth unit cell at $T=0$ is calculated from $G_{jn,jn}$. The formula for the top S layer, $N_{j1,j1}$, is very complicated, but it has the same structure as the right-hand side of the gap equation, namely, that there is an additional BCS-like contribution from the surface band with Δ_1 as the energy gap. Since $\Delta_1>\Delta$, which is the bulk OP, and the fact that the main peak in the bulk DOS falls at nearly one-half of Δ, the surface DOS would exhibit gap features at nearly twice the energy as the bulk DOS. In Fig. 6 we compare the top layer DOS with that of the bulk superconductor. Panel (B) shows the bulk DOS in Fig. 3, which is the limit of $N_{j1}(\omega)+N_{j2}(\omega)$ for $j\to\infty$. Panel (A) is the DOS of the top layer, $N_{11}(\omega)$, which has only one set of peaks at a much larger gap value. There is only a hint of the bulk DOS in the background, indicating that the top layer is

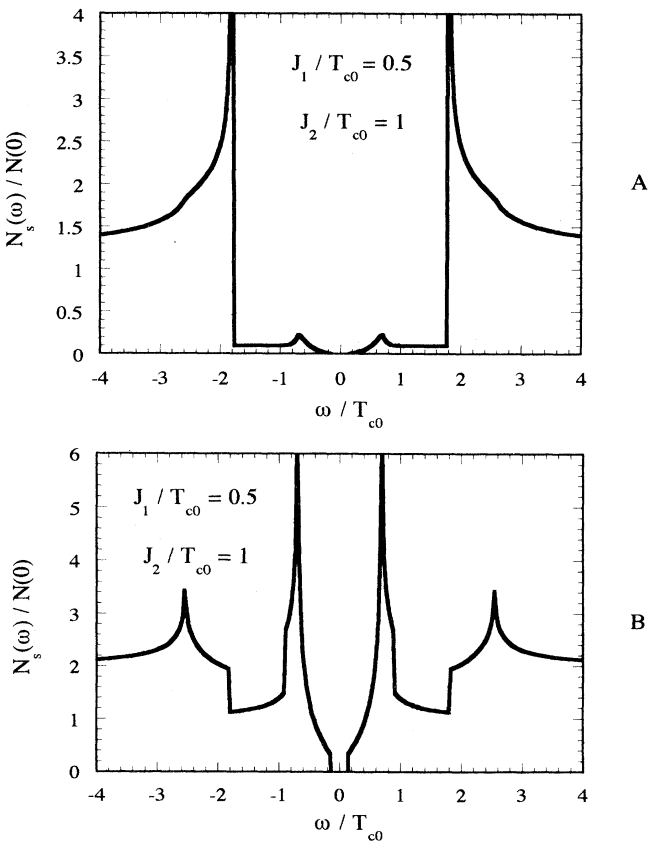

FIG. 6. The DOS curve in the superconducting state for the top S layer (A) compared with that of the bulk (B) for the model in Fig. 1.

effectively isolated from the rest of the system, and justifying the local approximation. We also performed similar calculations for $J_1 \geq J_2$, for which there is no surface band, and found that Δ_1 is only slightly enhanced and the DOS is indistinguishable from that of a bulk superconductor. Further discussion of the physical consequences of our findings will be the subject of Sec. V.

Equally interesting is the case where the top layer of the semi-infinite solid is nonsuperconducting but carries a surface state. The gap equation for the S layer in the jth unit cell is similar to Eq. (82) except that the factor $N_{j1}(k_z)$ is replaced by N_{j2} in Eq. (67). Numerical calculations show that even the energy gap Δ_1 of the S layer closest to the surface has essentially the bulk value. The DOS curve of the top N layer, shown in Fig. 7, exhibits the surface state contribution in the form of a uniform background of the value $N(0)(1-r^{-2})$. The physical significance of this result will also be discussed in Sec. V.

IV. THE THREE- AND FOUR-LAYER MODELS

The one- and two-layer models are oversimplifications of most real high-T_c materials. The most important materials, YBCO and BSCCO, both have two superconducting CuO_2 layers in a unit cell. In addition, YBCO has a conducting CuO chain layer and BSCCO has two BaO layers in a unit cell which are either conducting or semiconducting. Therefore, we need to extend our findings of surface state effects to models with more than two layers in a unit cell. A schematic diagram of a three-layer model is shown in Fig. 8. It has two S layers and one N layer in a unit cell. Inversion symmetry of the crystal demands that the two hopping integrals between the N layer and its two adjacent S layers be equal, i.e., $J_2 = J_3$ in Fig. 8. In addition, the N layer has a distinct electronic structure from the S layers, and we simulate this by offsetting the two-dimensional energy band of the N layer by an amount ϵ_0 from that of the S layers. The c-axis repeat distance is denoted by s.

The present authors have reported detailed analyses of the superconducting properties of three-layer and four-layer models in the strong hopping limit.[26] It was found that in general the DOS curves possess structures inside the main peaks due to the band dispersion in the c-axis direction. The formulation of the general hopping problem is rather complicated, but by analogy with the two-layer problem, we conclude that there should be additional peaks in the DOS curves due to interband pairing. For instance, there are three bands in the three-layer model with three distinct interband pairing possibilities. Consequently, the DOS curve is expected to have considerably more complex structure than that of the two-layer model. Figure 9 shows a typical DOS curve for the three-layer model. The curve has been folded with a resolution function whose width is approximately $0.05T_{c0}$ to simulate ac-

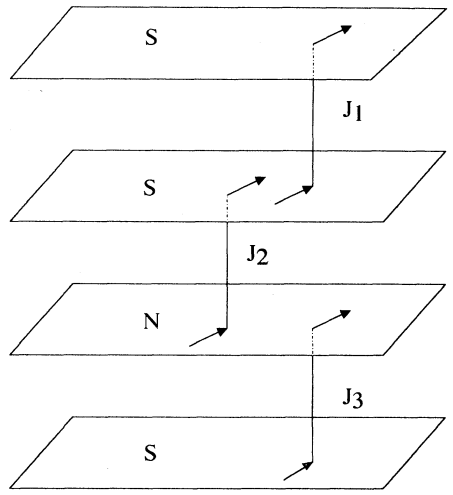

FIG. 8. The unit cell of a three-layer model. Inversion symmetry requires that certain hopping integrals be equal, e.g., $J_2 = J_3$ in this example.

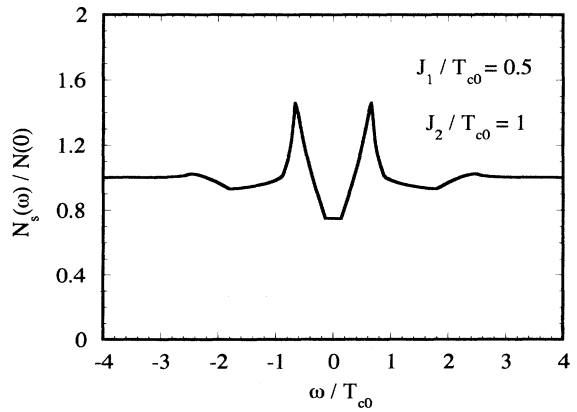

FIG. 7. The DOS curve of the top N layer of a semi-infinite system whose top layer is nonsuperconducting but carries a surface state.

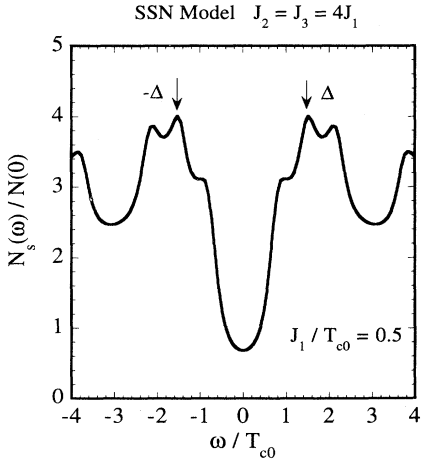

FIG. 9. The bulk DOS curve in the superconducting state for a three-layer model with two S layers and one N layer per unit cell. The model parameters are $J_1 = J_2 = 2T_{c0}$, $J_3 = 0.5T_{c0}$, and $\epsilon_0 = 0$, where T_{c0} is the critical temperature with all hopping turned off. The gap features are artificially broadened by $\delta = 0.05T_{c0}$ to simulate experimental resolution.

tual experiments. The shoulders inside the inner peaks have been seen in the junction tunneling data of Gurvitch *et al.* and Valles *et al.*[8]

It is too tedious to solve the surface superconductivity problem in detail. We can, nevertheless, take advantage of what we have learned from our previous analyses of the simpler models to draw definitive conclusions about possible surface effects. It was shown that the energy gap on the top S layer is enhanced provided that (1) a surface band exists whose charge density is concentrated in the top layer, and (2) the energy of the surface band does not contain the c-axis band energy which causes depairing. We will apply these two criteria on two models depicted in Fig. 10. The model (A) has an S layer on the top followed by an N layer. The third layer in the unit cell is an S layer below the N layer. The model (B) has an N layer on the top followed by two S layers.

We begin our discussion of surface state effects by examining the bulk bands because, as shown in Sec. III B, the band structure determines the important physical properties of the surface states. The band Hamiltonian for model (A) is

$$H_0=\sum_{\mathbf{k}\sigma}\sum_{j=1}^{\infty}[\xi_0(\mathbf{k})\psi_{j1\sigma}^{\dagger}\psi_{j1\sigma}+(\xi_0(\mathbf{k})+\epsilon_0)\psi_{j2\sigma}^{\dagger}\psi_{j2\sigma}+\xi_0(\mathbf{k})\psi_{j3\sigma}^{\dagger}\psi_{j3\sigma}]$$
$$+\sum_{j\mathbf{k}\sigma}[J_1\psi_{j1\sigma}^{\dagger}\psi_{j2\sigma}+J_2\psi_{j2\sigma}^{\dagger}\psi_{j3\sigma}+J_3\psi_{j3\sigma}^{\dagger}\psi_{j+1,1\sigma}+\text{H.c.}]\ . \tag{85}$$

Inversion symmetry requires that the hopping integrals satisfy the relation $J_1=J_2$. The first step in the search for surface bands is to determine the bulk band structure. This is done by solving for the zeros of the inverse of the bulk Green's function in the normal state, given by

$$\hat{G}^{-1}(k,\omega)=\begin{bmatrix}\omega-\xi_0(\mathbf{k}) & J_1 & J_3e^{-ik_zs}\\ J_1 & \omega-\xi_0(\mathbf{k})-\epsilon_0 & J_1\\ J_3e^{ik_zs} & J_1 & \omega-\xi_0(\mathbf{k})\end{bmatrix}. \tag{86}$$

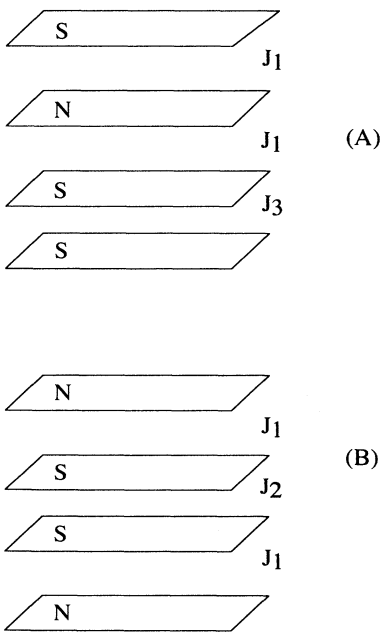

FIG. 10. A schematic drawing of two semi-infinite three-layer models under consideration. The model (A) has an S layer on top followed by one N layer and one S layer. Symmetry requires that $J_2=J_1$. The model (B) has an N layer on top followed by two S layers, with $J_3=J_1$ by symmetry.

The problem reduces to the solution of a cubic equation; the resulting energy bands are

$$\Omega_n(k)=\xi_0(\mathbf{k})+\omega_n(k_z)\ ,$$

for $n=1,2,3$. The c-axis part $\omega_n(k_z)$ forms three bulk energy bands shown in Fig. 11, with band gaps at $k_z=0$ and $k_z=\pi/s$. Surface states may exist in one or both of the band gaps.

The solution of the surface problem is similar to but much more complex than the two-layer model problem. We will give the results of this calculation without showing algebraic details. For sufficiently large and positive ϵ_0, the most likely location for a surface band is in the gap at $k_z=0$. The energy of this band is

$$\Omega_s(k)=\xi_0(\mathbf{k})+\omega_0\ , \tag{87}$$

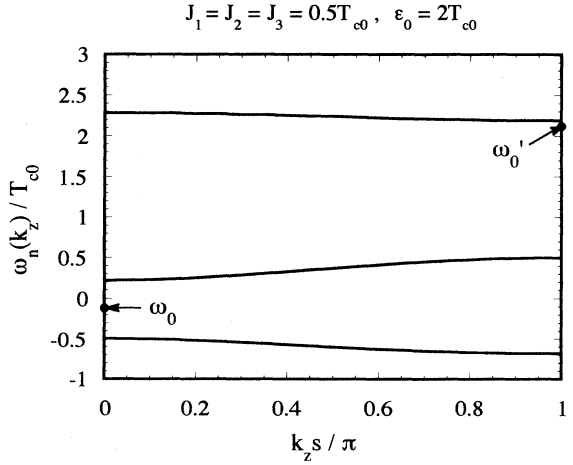

FIG. 11. The c-axis part $\omega_n(k_z)$ of the normal-state bulk band structure of the three-layer model in Fig. 8. The model parameters are $J_1=J_2=J_3=0.5T_{c0}$ and $\epsilon_0=2T_{c0}$. The point ω_0 marks the energy and momentum position of the surface state of model (A) in Fig. 10, and ω_0' is the position of the surface state of model (B).

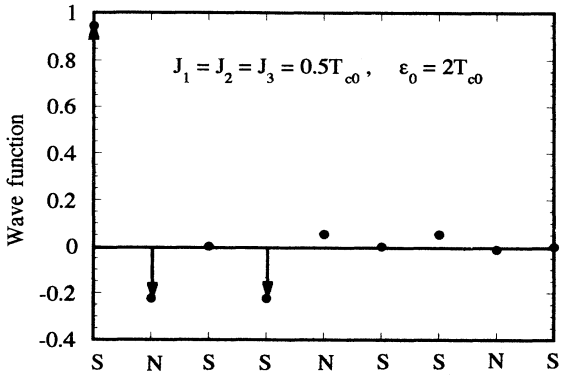

FIG. 12. The wave function of the surface band for the model in Fig. 10A plotted versus the layer index. The model parameters are shown in the graph. The wave function is relatively small but nonvanishing on the normal layers.

where the c-axis part of the band energy is

$$\omega_0 = -\tfrac{1}{2}[\sqrt{\epsilon_0^2 + J_1^2} - \epsilon_0] \ . \tag{88}$$

It can be seen that ω_0 can be quite small if ϵ_0 is sufficiently greater than J_1, as depicted in Fig. 11. The wave function of this surface state is sketched in Fig. 12. Its spectral weight on the top S layer is

$$\rho_{11} = \left[1 - \left[\frac{\omega_0}{J_3}\right]^2\right] \Big/ \left[1 + \left[\frac{\omega_0}{J_1}\right]^2\right] \ . \tag{89}$$

For the next N layer,

$$\rho_{12} = \frac{\omega_0}{J_1}\rho_{11} \ . \tag{90}$$

The third S layer has $\rho_{13} = 0$. While this band of surface states does not completely avoid the N layer as the two-layer case, its spectral density can be sufficiently small to cause little depairing. Under this circumstance, the surface superconductivity is expected to be enhanced. The surface band crosses the Fermi level in a surface between the two sheets of Fermi surfaces of the S layers, as was simulated in the two-layer model discussed in the last section. Unlike the two-layer model, the formation of this surface band depends sensitively on the N layer band offset ϵ_0, rather than on the hopping parameters. This requirement seems to be physically more realistic.

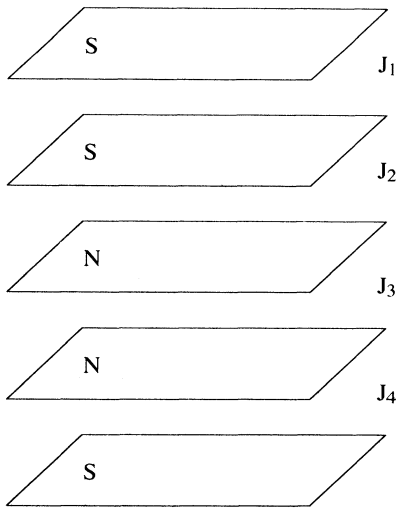

FIG. 13. A schematic drawing of a semi-infinite four-layer model whose two topmost layers are S followed by two N layers. Inversion symmetry of the crystal demands that the hopping integrals satisfy the relation $J_2 = J_4$.

Similarly, we find that model (B) yields a surface state at the point ω_0' in Fig. 11, where

$$\omega_0' = \tfrac{1}{2}[\sqrt{\epsilon_0^2 + J_1^2} + \epsilon_0] \ . \tag{91}$$

This surface state does not enhance superconductivity because its wave function is concentrated mainly in the N layer. Unlike the two-layer model, where we have found it necessary to break the inversion symmetry, i.e., $J_1 \neq J_2$, in order to find a surface state, both models (A) and (B) are symmetric under inversion and have surface states.

We have also examined a possible model that has two S layers on top of the N layer. No surface state has been found. If the band offset ϵ_0 is negative, the surface state ω_0 for model (A) occurs at $k_z = \pi/s$ and ω_0' for model (B) occurs at $k_z = 0$. The surface state effects remain the same in both cases.

The four-layer model contains too many parameters to be algebraically tractable. To keep the discussion on the accessible level, we consider a model which contains two S layers and two N layers in a unit cell, as shown in Fig. 13. We also ignore the normal layer band offset so that the band Hamiltonian is relatively simple:

$$H_0 = \sum_{\mathbf{k}\sigma} \sum_{j=1}^{\infty} \sum_{n=1}^{4} \xi_0(\mathbf{k}) \psi_{jn\sigma}^{\dagger} \psi_{jn\sigma} + \sum_{j\mathbf{k}\sigma} [J_1 \psi_{j1\sigma}^{\dagger} \psi_{j2\sigma} + J_2 \psi_{j2\sigma}^{\dagger} \psi_{j3\sigma} + J_3 \psi_{j3\sigma}^{\dagger} \psi_{j,4\sigma} + J_4 \psi_{j4\sigma}^{\dagger} \psi_{j+1,1\sigma} + \text{H.c.}] \ . \tag{92}$$

Inversion symmetry imposes the constraint $J_2 = J_4$ on the model parameters. The bulk bands are given by

$$\Omega_n(k) = \xi_0(\mathbf{k}) + \omega_n(k_z) \ , \tag{93}$$

for $n = 1-4$. The c-axis part $\omega_n(k_z)$ is given by

$$\omega_n(k_z) = \pm[A \pm \sqrt{A^2 - B}\,]^{1/2} \ , \tag{94}$$

where

$$A = \tfrac{1}{2}(J_1^2 + J_2^2 + J_3^2 + J_4^2) \ , \tag{95}$$

and

$$B = J_1^2 J_2^2 + J_3^2 J_4^2 + 2J_1 J_2 J_3 J_4 \cos k_z s \ . \tag{96}$$

The c-axis part of the bulk bands, plotted in Fig. 14, has

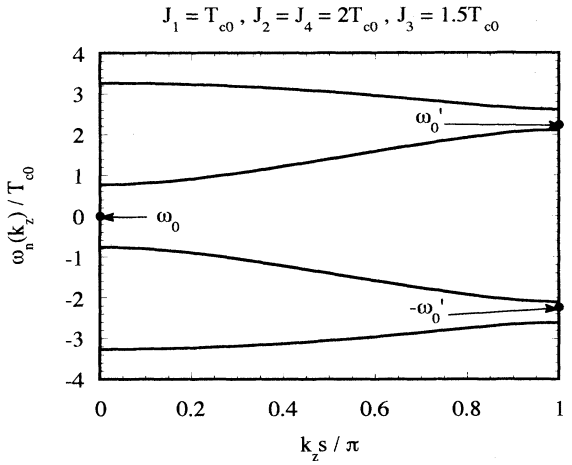

FIG. 14. The c-axis part $\omega_n(k_z)$ of the normal-state bulk band structure of the four-layer model in Fig. 13. The model parameters are shown in the figure. The points ω_0 and $\pm\omega_0'$ indicate possible positions of surface states.

one band gap at $k_z=0$ and two gaps at $k_z=\pi/s$. Surface states may be stable inside these band gaps.

Under the condition $J_2J_4>J_1J_3$, we find a surface state with energy $\omega_0=0$ at $k_zs=i\kappa$ where $e^{\kappa}=J_2J_4/J_1J_3$. The wave function of this state, sketched in Fig. 15, is concentrated on the top S layer. It enhances superconductivity on the surface layer according to the criteria discussed earlier in this section. Two other surface states with energies $\pm\omega_0'$, where $\omega_0'=\sqrt{J_1^2+J_2^2}$, are stable under the condition $J_1>J_3$. We will not discuss these states further because they do not enhance surface superconductivity. Again, it is not necessary to break the inversion symmetry in order to find surface states in the four-layer model.

Our discussion of surface state effects has been based on simple tight-binding models whose model parameters remain the same on the surface. In reality, the model parameters often change due to surface relaxation and surface reconstruction. The proper way to locate the surface

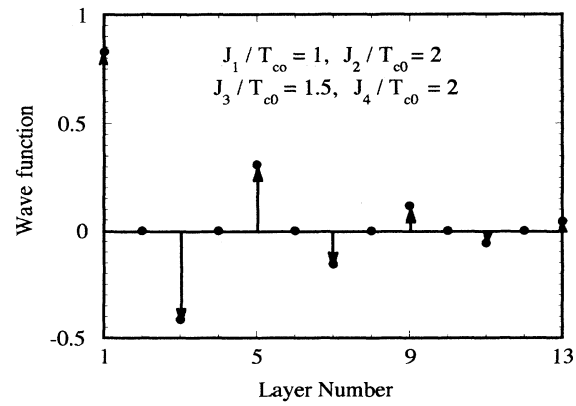

FIG. 15. The wave function of the surface state at ω_0 in Fig. 14. The spectral density of this state is concentrated in the top S layer.

states on a real solid surface is to perform *ab initio* band calculations, such as that done by Lindroos and Bansil[27] for $Nd_{2-x}Ce_xCuO_4$ (NCCO). They find surface states on two Nd terminated surfaces. The energetic position and $k_{\parallel}$ dispersion of one of these states are consistent with existing photoemission data.[28] This lends support to our contention that photoemission signals are often dominated by surface state contributions,[15] a point which will be expanded further in the next section. Furthermore, they show that the surface states couple almost exclusively with p-polarized photons, such that a simple test suffices to determine whether a photoemission signal comes from bulk or surface states. They also report that no surface state has been found on YBCO surfaces, a result which explains why, in spite of repeated efforts, the superconducting gap has not been observed by photoemission on this material.

V. DISCUSSION

In this final section we discuss the physical consequences of our findings concerning the effects of surface bands on the observed superconducting properties of layered superconductors. Of particular significance are two surface-sensitive experiments, namely, tunneling and photoemission.

The presence of surface states can affect the outcome of tunneling measurements of the gap, depending upon the type of junction and the tunneling surface geometry. With point-contact tunneling along the a,b axes, tunneling into the bulk S and N layers leads to a fairly accurate measurement of the bulk tunneling DOS, as pictured in panel (B) of Fig. 6. For point-contact tunneling with the tip along the c axis, different results are expected due to surface effects. Such differences are most pronounced when the tip is near a crystal growth seam the height of one c-axis unit cell. In this case, it is likely that the tunneling current comes predominantly from within the top S layer (perpendicular to the c axis). Since the electronic structure of this layer is dominated by surface state effects, the resulting DOS curve is expected to resemble that in panel (A) of Fig. 6, or with that in Fig. 7, depending on whether the top layer is an S or an N layer, respectively. With junction tunneling along the c axis, the barrier often reacts chemically with the top surfaces (e.g., removing oxygen), destroying the surface state, although an interface state, which has the same physical properties as a surface state, can be formed. Thus, junction tunneling along both the a,b and c-axis directions should give similar (although not necessarily identical) bulklike DOS results, provided that good junctions can be prepared and the tunneling current penetrates more than a unit cell depth. Break junction results along the c axis would be sensitive to surface states, whereas those along the a,b axes would not.

Both point-contact and junction tunneling experiments have been reported for BSCCO in the c direction. The junction tunneling results of Tao *et al.*[6] reveal a gap at approximately 40 meV, in agreement with the a,b plane tunneling result, 35 meV reported by Chen and Ng.[6] Both papers show tunneling characteristics with V-

shaped bottoms. The point-contact result reported by Hasegawa *et al.*[7] shows tunneling curves with flat bottoms and gap values in excess of 50 meV, close to the value of 55 meV obtained by Mandrus *et al.*[7] for an a,b-axis break junction. Those authors did not observe any c-axis break junction gap structure, but that may be a feature of the cleaved Bi-O surface layer on each junction half. Two recent reports on point-contact tunneling measurements along the c axis of BSCCO lend support to published data. Murakami and Aoki examined a region of the (001) surface of a BSCCO single crystal, in which the cleave resulted in a step the overall height of one-half of a c-axis unit cell.[29] On the top and bottom portions of the step, the Bi-O surface was exposed and the step exhibited a semiconducting gap of about 100 meV when the tip was far from the surface. As the tip approached (and may have crashed) the Bi-O surface, this semiconducting gap evolved into a superconducting gaplike structure, with a V-shaped bottom and rather sharp peaks at 40 meV. On the other hand, when the tip was placed above the intermediate step region (roughly halfway between the Bi-O surfaces), the tunneling characteristics were very different. In these cases, the tunneling current did not depend upon the tip position, either on its height or its location above this step, and showed peaks at ± 40 meV, but flat bottoms of width 20 meV. Similar results were also seen by Hasegawa *et al.*[30] Assuming the most likely scenario that the intermediate step corresponded to a CuO_2 plane, these results strongly suggest that proximity coupling between the top (narrow gap semiconducting) Bi-O layer with the superconducting CuO_2 layers is occurring, and the superconductivity within the CuO_2 layers is nodeless, or s-wave like.

The situation with YBCO is quite similar. The junction tunneling data of Gurvitch *et al.*[8] revealed a gaplike, temperature-dependent feature at 4–5 meV, with a large zero-bias conductance, very similar to the DOS curve shown in Fig. 7 for a surface (or interface) state on the top N layer. This behavior was also seen with c-axis junctions on YBCO (001) films.[31] On the other hand, point-contact tunneling along the c axis[6,29] of some (001) films gave semiconducting gaplike behavior when the tip was far from the surface, but superconducting gaplike structures at ± 20 meV with a large zero-bias conductance when the tip was closer to the surface. On other YBCO (001) films (grown at relatively low temperatures), however, a clear superconducting gap of 40 meV with an extremely flat bottom and low zero-bias conductance (less than 1% of the background) was seen. Such behavior was also seen when the tip was along a seam comprising a step of a c-axis unit cell in height (and hence involved tunneling primarily into the CuO_2 layers). Point-contact tunneling into the a,b axes of (110) YBCO films[32] gave V-shaped gaplike features with large zero-bias conductances, indicative of the relative importance of the normal CuO chains. Hence, both the tunneling results for BSCCO and YBCO are consistent with our model of s-wave superconductivity in the CuO_2 layers, with proximity coupling to adjacent N layers, and with surface states on the top atomic layer on the (001) surface.

In our model no surface band can exist in a system with one S layer per unit cell and no N layers. The model can be realized if the interstitial region between S layers is insulating, with large insulating gap. Band calculations predict such an electronic structure for underdoped $HgBa_2CuO_{4+\delta}$ (Hg1201).[33] With increasing doping of Hg1201, the band gap decreases, until at overdoped Hg1201, the Hg-O chains hybridize with the CuO_2 planes.[33] We predict that, for underdoped and perhaps optimally doped Hg1201, there should be no difference between the surface and bulk DOS, and both are BCS like for intralayer s-wave pairing. This prediction is in agreement with the point-contact tunneling measurements on Hg1201 by Chen *et al.*,[34] which showed the strongest point-contact tunneling evidence for s-wave superconductivity in a cuprate. We have not investigated the possibility of surface states in the case in which the interstitials were narrow-gap semiconductors, having energy bands near the Fermi surface. The *ab initio* calculation of Lindroos and Bansil[27] for NCCO fills this void nicely. They found that one surface state on a top Nd surface was consistent with photoemission experiments[28] on NCCO. Such surface states might account for the point-contact tunneling results of Zasadzinski *et al.*,[35] which showed rather BCS-like behavior but with a nonvanishing zero-bias conductance and a U-shaped bottom, somewhat different from that observed in Hg1201.

Photoemission experiments are also vulnerable to surface state effects.[15] While the incident photons may penetrate several or many unit cells into the sample, the outgoing electrons escape from the top few atomic layers. The situation is especially acute in cases where the c-axis transport have considerable incoherent character such that the escaping photoelectrons will only contain phase-coherent information from the top single atomic layer. Also, in photoemission experiments on high-T_c superconductors, one does not see the gap directly, but infers the existence of a gap by a shift of the peak as one traverses T_c. All such experiments are carried out on cleaved (001) surfaces, which are most sensitive to surface state effects. In case the surface conducting layer is an N layer, the DOS of the top layer is gapless and would result in no observed shift in spectral peak. Indeed, all angle-resolved photoemission experiments on YBCO, oxygen-deficient YBCO, $YBa_2Cu_4O_8$, and NCCO have failed to see the superconducting gap. While in NCCO the failure to observe the gap might be due to the smaller value of T_c (and hence the gap), in the other materials the T_c values were comparable to that of BSCCO, the *only* material in which the apparent observation of the superconducting gap by angle-resolved photoemission spectroscopy (ARPES) experiments has been reported.

For YBCO the Fermi surface predicted by Pickett *et al.*[36] contains two CuO_2 bands, a CuO chain band, and a "post" and near the S point. Whereas early ARPES measurements on YBCO (Ref. 37) claimed to observe the Fermi surface at the S point and part of the chain band, the only Fermi-surface crossings observed in that experiment, which proved to be correct in light of later experiments, were the two CuO_2 Fermi-surface crossings.[38] The CuO chain band was only observed in 2D-ACAR

(two-dimensional angular correlation of annihilation radiation) (positron annihilation) experiments,[39] and the Fermi surface near the S point may have been seen in de Haas–van Alphen "bomb" experiments.[40] Similarly, the existence of the Fermi surface in the ET-based [ET: bis(ethylenedithio)tetrathiafulvalene] organic superconductors has been well established by de Haas–Shubnikov oscillations[41] and de Haas–van Alphen measurements[42] but not in ARPES experiments.[43] Hence, there are probably a number of reasons why some or all pieces of the Fermi surface of a material might be difficult to observe in ARPES experiments. Subsequently, Gofron[44] was able to observe two bands near E_F close to the Y-S and X-S directions, but not along the Γ-S direction. The fact that no one has observed any difference in the quasiparticle dispersions above and below T_c is consistent with our surface picture, that either the top surface is semiconducting or normal, or that is supports no surface state.[27]

Similar two-band Fermi surfaces were predicted[45] in a calculation of the electronic structure of BSCCO, both with and without mixing of the Bi-O bands with the CuO_2 bands. Dessau *et al.* claimed to observe both CuO_2 bands, which touched each other along the Γ-X and Γ-Y lines as predicted,[45] due to the high crystal symmetry of these directions.[46] However, recent measurements by Ding *et al.*[47] have disputed this. Furthermore, there have been reports by Aebi *et al.*[48] and by Kelley *et al.*[49] of similar experiments such that the Fermi surfaces, superconducting gap functions, and interpretations extracted from these four groups all differ from each other. While none of these measurements claimed to be able to see the Bi-O band, it is possible that the top surface Bi-O layer is a narrow-gap semiconducting layer, consistent with the tunneling measurements.[6,29,30] The Bi-O bands in the bulk of the sample may cross the Fermi energy as predicted,[45] but the ARPES experiments do not probe deep enough to see even the second Bi-O layer. To complicate the situation further, the Bi-O layers exhibit an incommensurate lattice distortion,[50] which greatly affects the analysis and may account for some of the differences in the interpretation of experimental results from the different groups. There is an additional materials problem with BSCCO, that it is not a stoichiometric compound. Many physical properties on different compounds may appear at first sight to be rather similar, yet differences in other properties may lurk in the background. For instance, most samples have T_c values in the range 80–85 K and semiconductinglike c-axis resistivity characteristics, but crystals with T_c values of 97 K and metallic c-axis resistivities have been reported.[51]

With these caveats in mind, we shall try to present a possible interpretation of some, if not all, of the ARPES experiments on BSCCO. In the theory[45] and in some of the experiments,[44,46,48] the CuO_2 bands touch along Γ-X and Γ-Y lines. Figure 16 shows a possible manifestation of this electronic structure, in which J_1 and J_2 are functions of k_x, k_y such that

$$J_1(\mathbf{k}) = J_2 - J' |\cos k_x a - \cos k_y a| \ , \tag{97}$$

with $J' > 0$ so that $J_1(\mathbf{k}) < J_2$ over the two-dimensional Brillouin zone except at four points where they are equal. At these points the two bulk bands and their Fermi surfaces touch at $k_z = \pi/s$ as in Refs. 1, 46, and 48. Assuming that the top layer is an S layer, we find that the spectral weight of the surface states vanishes at just these points. Hence, the apparent vanishing of the gap at these points in BSCCO (Ref. 1) is consistent with the vanishing of the spectral weight of the surface states in an s-wave superconductor. The fact that the apparent anisotropy disappears once the surface is contaminated[1] also suggests that the entire effect is linked to the surface band rather than the bulk band.

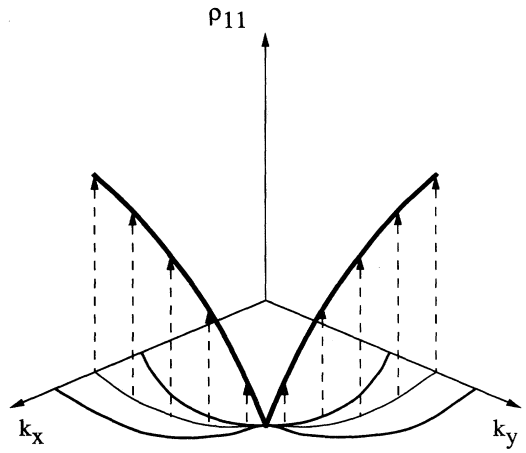

FIG. 16. The distribution of the surface state charge density on the top layer of a two-layer system where the hopping integrals are dependent on k_x, k_y such that $J_1 = J_2$ at a set of points in the two-dimensional Brillouin zone. The surface state vanishes at these points.

The hopping parameters may depend sensitively on the stoichiometry of the material. If in some samples the leading term on the right-hand side of Eq. (97) is less than J_2, the two sheets of Fermi surface will not touch even along the Γ-X and Γ-X lines, resulting in the observation that the gap is small there but nonvanishing, as reported in Ref. 1 for some samples. In a similar manner, if the leading term is slightly greater than J_2, the two sheets will cross at pairs of points on either side of the Γ-X and Γ-Y symmetry lines and the measured gap appears to be small between these crossings, as in Refs. 47 and 52.

Our findings for the three-layer model may shed further light on some intriguing properties of YBCO. Since ARPES experiments have failed to observe a superconducting gap on either fully oxygenated or oxygen-deficient YBCO, we interpret this as arising from the top layer being an N layer (or perhaps a pair of S layers), for which the superconducting DOS would be gapless.

Finally, another possible manifestation of surface states in photoemission experiments might be the observation of "extended van Hove singularities," which are sharp quasiparticle peaks near the Fermi energy, as observed by Gofron *et al.*[53] in $YBa_2Cu_4O_8$ and by Dessau *et al.*[46] in a $Bi_2(Sr_{0.97}Pr_{0.03})_2CuO_{6+\delta}$ (Bi2201). In particular, Figs. 4(b) and 4(c) of Ref. 53 show that the extra quasiparticle

peaks appear halfway between the bulk quasiparticle bands, as expected for surface states in our model. One ought to consider the possibility that these so-called "extended van Hove singularities" might really just be surface states, and hence might not be the primary source for the high-T_c values of the cuprates.

In conclusion, both the variety of tunneling results and the apparent gap anisotropy observed with photoemission on high-T_c superconductors are consistent with s-wave superconductivity, provided that one takes the surface states into account. We would urge similar experiments be performed on underdoped and possibly optimally doped Hg1201, for which there is only one CuO_2 derived band and no normal layers,[33] and hence such surface states are not expected.

ACKNOWLEDGMENTS

The authors are indebted to A. A. Abrikosov, O. K. Andersen, R. Benedek, J. C. Campuzano, K. J. Gofron, K.-M. Ho, Marko Ledvij, D. H. Lowndes, E. W. Plummer, Z.-X. Shen, J. F. Zasadzinski, and D. M. Zehner for encouragement and informative discussions. One of the authors (S.H.L.) would like to thank Professor L. Sham and Professor R. Dynes for their hospitality. This research was supported by the U.S. Department of Energy, Division of Basic Energy Sciences, under Contract No. DE-AC005-84OR21400 with Martin Marietta Energy Systems, Inc., and No. W-31-109-ENG-38. This work was done in part at Oak Ridge National Laboratory, Oak Ridge, TN.

[1]Z.-X. Shen *et al.*, Phys. Rev. Lett. **70**, 1553 (1993).
[2]D. A. Wollman *et al.*, Phys. Rev. Lett. **71**, 2134 (1993); **74**, 797 (1995).
[3]C. C. Tsuei *et al.*, Phys. Rev. Lett. **75**, 593 (1994).
[4]A. Mathai, Y. Gim, R. C. Black, A. Amar, and F. C. Wellstood, Phys. Rev. Lett. **74**, 4523 (1995).
[5]W. N. Hardy *et al.*, Phys. Rev. Lett. **70**, 1553 (1993); D. A. Bonn *et al.*, Phys. Rev. B **47**, 11 314 (1993).
[6]H. J. Tao *et al.*, Phys. Rev. B **45**, 10 622 (1992); Q. Chen and K.-W. Ng, *ibid.* **45**, 2569 (1992).
[7]T. Hasegawa *et al.*, J. Phys. Chem. Solids **53**, 1643 (1992); D. Mandrus *et al.*, Nature **351**, 460 (1991).
[8]M. Gurvitch *et al.*, Phys. Rev. Lett. **63**, 1008 (1989); J. M. Valles, Jr. *et al.*, Phys. Rev. B **44**, 11 986 (1991).
[9]A. G. Sun *et al.*, Phys. Rev. Lett. **72**, 2267 (1994).
[10]P. Chaudhari and S.-Y. Lin, Phys. Rev. Lett. **72**, 1084 (1994).
[11]J. Buan *et al.*, Phys. Rev. Lett. **72**, 2632 (1994); O. Valls, Bull. Am. Phys. Soc. **40**, 2 (1995).
[12]S. H. Liu and R. A. Klemm, Phys. Rev. B **48**, 4080 (1993).
[13]S. H. Liu and R. A. Klemm, Phys. Rev. B **48**, 10 650 (1993).
[14]S. H. Liu and R. A. Klemm, Physica C **216**, 293 (1993).
[15]S. H. Liu and R. A. Klemm, Phys. Rev. Lett. **73**, 1019 (1994).
[16]R. A. Klemm and S. H. Liu, Phys. Rev. Lett. **74**, 2343 (1995).
[17]H. Svensmark and L. M. Falicov, Phys. Rev. B **40**, 201 (1989).
[18]T. Giamarchi, M. T. Béal-Monod, and O. T. Valls, Phys. Rev. B **41**, 11 033 (1990); S. W. Pierson, and O. T. Valls, *ibid.* **45**, 2458 (1992).
[19]K. B. Efetov and A. I. Larkin, Zh. Eksp. Teor. Fiz. **68**, 155 (1975) [Sov. Phys. JETP **41**, 76 (1975)].
[20]We can justify this seemingly *ad hoc* procedure by contour integration in the complex ξ_0 space.
[21]A. A. Abrikosov, Physica C **182**, 191 (1991).
[22]R. A. Klemm and S. H. Liu, Physica C **176**, 189 (1991); Phys. Rev. B **44**, 7526 (1991).
[23]H. Bando, S. Kashiwaya, H. Tokumoto, H. Anzai, N. Kinoshita, and K. Kajimura, J. Vac. Sci. Technol. A **8**, 479 (1990).
[24]O. K. Andersen, A. I. Liechtenstein, O. Rodriguez, I. I. Mazin, O. Jepsen, V. P. Antropov, O. Gunnarsson, and S. Gopalan, Physica C **185-189**, 147 (1991).
[25]For a comprehensive review of the physics of surface states, see J. E. Inglesfield, *Electronic Properties of Surfaces* (Adam Hilger, Bristol, 1984), pp. 1–69.
[26]S. H. Liu and R. A. Klemm, Phys. Rev. B **45**, 415 (1992).
[27]M. Lindroos and A. Bansil (unpublished).
[28]D. M. King *et al.*, Phys. Rev. Lett. **73**, 3298 (1994); **70**, 3159 (1993).
[29]H. Murakami and R. Aoki, J. Phys. Soc. Jpn. **64**, 1287 (1995).
[30]T. Hasegawa, M. Nantoh, M. Ogino, H. Sugawara, M. Kawasaki, H. Koinuma, and Kitazawa, J. Supercond. (to be published).
[31]A. S. Katz *et al.*, Appl. Phys. Lett. **66**, 105 (1995).
[32]M. Nantoh, T. Hasegawa, W. Yamaguchi, A. Takagi, M. Ogino, K. Kitazawa, M. Kawasaki, J. Gong, and H. Koinuma, J. Appl. Phys. **75**, 5227 (1994).
[33]D. L. Novikov and A. J. Freeman, Physica C **212**, 233 (1993).
[34]J. Chen *et al.*, Phys. Rev. B **49**, 3683 (1994); J. Chen, J. S. Zasadzinski, K. E. Gray, J. L. Wagner, D. G. Hinks, K. Kouznetsov, and L. Coffey, IEEE Trans. Appl. Supercond. (to be published).
[35]J. F. Zasadzinski *et al.*, J. Phys. Chem. Solids **53**, 1635 (1992).
[36]W. E. Pickett *et al.*, Phys. Rev. B **42**, 8764 (1990).
[37]J. C. Campuzano *et al.*, Phys. Rev. Lett. **64**, 2308 (1990).
[38]R. Liu *et al.*, Phys. Rev. B **45**, 5614 (1992).
[39]L. C. Smedskjaer and A. Bansil, J. Phys. Chem. Solids **53**, 1657 (1992).
[40]C. M. Fowler *et al.*, Phys. Rev. Lett. **68**, 534 (1992).
[41]K. Oshima *et al.*, Phys. Rev. B **38**, 938 (1988).
[42]J. Wosnitza *et al.*, Phys. Rev. Lett. **67**, 263 (1991).
[43]R. Liu *et al.*, Phys. Rev. B **51**, 6155 (1995).
[44]K. J. Gofron, Ph.D. thesis, University of Illinois at Chicago (1993); J. Phys. Chem. Solids **54**, 1193 (1993).
[45]S. Massida, J. Yu, and A. J. Freeman, Physica C **152**, 251 (1988).
[46]D. S. Dessau *et al.*, Phys. Rev. Lett. **71**, 2781 (1993).
[47]H. Ding, J. Z. Campuzano, A. F. Bellman, T. Yokoya, M. R. Norman, M. Randeria, T. Takahashi, H. Katayama-Yoshida, T. Mochiku, K. Kadowaki, and G. Jennings, Phys. Rev. Lett. **74**, 2784 (1995).
[48]P. Aebi *et al.*, Phys. Rev. Lett. **72**, 2757 (1994).
[49]R. J. Kelley *et al.*, Phys. Rev. Lett. **71**, 4051 (1993); R. J. Kelley *et al.*, Phys. Rev. B **50**, 590 (1994); J. Ma *et al.*, Science **267**, 862 (1995).
[50]R. L. Withers *et al.*, J. Phys. C **21**, 6067 (1988).
[51]T. Badèche, O. Monnereau, A. M. Ghorayeb, V. Grachev, and C. Boulesteix, Physica C **241**, 10 (1995).
[52]Z.-X. Shen, Bull. Am. Phys. Soc. **40**, 745 (1995).
[53]K. J. Gofron, J. C. Campuzano, A. A. Abrikosov, M. Lindroos, A. Bansil, H. Ding, D. Koelling, and B. Dabrowski, Phys. Rev. Lett. **73**, 3302 (1994); D. M. King *et al.*, *ibid.* **73**, 3298 (1994).